Biotechnology Reports 20 (2018) xxx–xxx

Contents lists available at ScienceDirect

Biotechnology Reports

journal homepage: www.elsevier.com/locate/btre

Increased fucoxanthin in *Chaetoceros calcitrans* extract exacerbates apoptosis in liver cancer cells via multiple targeted cellular pathways

Su Chern Foo[a,b], Fatimah Md. Yusoff[a,c,d,*], Mustapha Umar Imam[a,f], Jhi Biau Foo[a,g], Norsharina Ismail[a], Nur Hanisah Azmi[a,e], Yin Sim Tor[a,h], Nicholas M.H. Khong[a], Maznah Ismail[a]

[a] *Institute of Bioscience, Universiti Putra Malaysia, 43400 UPM, Serdang, Selangor Darul Ehsan, Malaysia*
[b] *School of Science, Monash University Malaysia, Jalan Lagoon Selatan, 47500, Bandar Sunway, Selangor Darul Ehsan, Malaysia*
[c] *The International Institute of Aquaculture and Aquatic Science, Universiti Putra Malaysia, 43400, UPM, Serdang, Selangor Darul Ehsan, Malaysia*
[d] *Department of Aquaculture, Faculty of Agriculture, Universiti Putra Malaysia, 43400 UPM, Serdang, Selangor Darul Ehsan, Malaysia*
[e] *Department of Cell and Molecular Biology, Faculty of Biotechnology & Biomolecular Sciences, Universiti Putra Malaysia, 43400 UPM, Serdang, Selangor, Malaysia*
[f] *Department of Medical Biochemistry, College of Health Sciences, Usmanu Danfodio University, Sokoto, Nigeria*
[g] *School of Pharmacy, Faculty of Health & Medical Sciences, Taylor's University, No. 1 Jalan Taylor's, 47500, Subang Jaya, Selangor Darul Ehsan, Malaysia*
[h] *School of Biosciences, Faculty of Health & Medical Sciences, Taylor's University, No. 1 Jalan Taylor's, 47500, Subang Jaya, Selangor Darul Ehsan, Malaysia*

ARTICLE INFO

Article history:
Received 8 October 2018
Received in revised form 14 November 2018
Accepted 3 December 2018

Keywords:
Chaetoceros calcitrans
Microalgae
Fucoxanthin
Rich fraction
Apoptosis
Gene expression

ABSTRACT

In this study, anti-proliferative effects of *C. calcitrans* extract and its fucoxanthin rich fraction (FxRF) were assessed on human liver HepG2 cancer cell line. Efficacy from each extract was determined by cytotoxicity assay, morphological observation, and cell cycle analysis. Mechanisms of action observed were evaluated using multiplex gene expression analysis. Results showed that CME and FxRF induced cytotoxicity to HepG2 cells in a dose and time-dependent manner. FxRF (IC_{50}: 18.89 $\mu g.mL^{-1}$) was found to be significantly more potent than CME (IC_{50}: 87.5 $\mu g.mL^{-1}$) ($p < 0.05$). Gene expression studies revealed that anti-proliferative effects in treated cells by *C. calcitrans* extracts were mediated partly through the modulation of numerous genes involved in cell signaling (*AKT1*, *ERK1/2*, *JNK*), apoptosis (*BAX, BID, Bcl-2, APAF, CYCS*) and oxidative stress (*SOD1*, *SOD2*, *CAT*). Overall, *C. calcitrans* extracts demonstrated effective intervention against HepG2 cancer cells where enhanced apoptotic activities were observed with increased fucoxanthin content.

1. Introduction

Hepatocellular (liver) cancer is increasing in incidence and mortality rates in many countries that previously reported low frequencies [1]. It is the sixth most common cancer worldwide and the second most common cause of death by cancer [2]. The liver plays an important role in the metabolism of exogenous substances and its cancerous growth can alter body internal environment due to its central role in metabolism. In most cancer cells, deregulated cell cycle as a result of mutation allows cells to skip cell cycle regulation and programmed cell death [3]. As a result, cancer cells fail to undergo apoptosis, which leads to increased cell survival and ultimately cancer metastasis [4].

To date, apoptosis remains the desired form of killing cancer cells as it involves a systematic series of regulated cell events to perform cellular suicide without triggering inflammation. Some liver chemotherapeutic agents like doxorubicin are effective in inducing apoptosis [5] but its side effects limit consumer acceptance [6]. These concerns are driving the search for new anti-cancer agents. Approximately 25% of the current anti-cancer drugs are derived from plant compounds and another 25% chemically modified from natural products [7]. In recent years, much attention has focused on effective marine-derived bioactive compounds [8,9]. Accordingly, Ziconotide (Prialt®), a peptide from the tropical cone snail was the first anti-pain marine drug, while trabectedin (Yondelis®) was approved for soft tissue sarcoma by the European Union in 2007 [10]. However, it was reported that

Abbreviations: MTT, 3-(4,5-dimethylthizol-2-yl-2,5 diphenyltetrazolium bromide); RNA, ribonucleic acid; DMSO, dimethyl sulfoxide; CME, crude methanolic extract; FxRF, fucoxanthin rich fraction; PBS, phosphate buffered saline; mg FX.g^{-1} extract, milligram of fucoxanthin per gram of *Chaetoceros calcitrans* extract.

* Corresponding author at: Institute of Bioscience, Universiti Putra Malaysia, 43400 UPM, Serdang, Selangor Darul Ehsan, Malaysia.
E-mail address: fatimahyus@gmail.com (F.M. Yusoff).

https://doi.org/10.1016/j.btre.2018.e00296

among marine bioactives, those from microalgae were puzzlingly the least explored [11]. This, in turn, left a huge arsenal of unexplored microalgae as sources of evidence-based marine medicines for the development of natural and novel anti-cancer drugs.

Diatoms from the class Bacillariophyceae e.g. *Phaeodactylum tricornutum, Skeletonema costatum, Chaetoceros calcitrans* have the advantage of being sustainable bioactive sources of carotenoids, phenolic compounds and essential fatty acids [12,13]. Compared to terrestrial plants, they have short generation cycles and adaptability to grow in closely monitored photobioreactor systems. This allows for a stable supply of natural compounds with consistent quality throughout the year. Natural antioxidants (e.g. carotenoids and phenolic acids) from microalgae are not just capable of free radical scavenging [14] but also has the potential as anti-cancer agents. They are capable of targeting multiple cell signaling pathways [15,16]. In particular, algae from *Bacillariophyceae and Phaeophyceae* contain a unique light-harvesting pigment, fucoxanthin, that has been proven to exhibit anti-proliferative activities against cancer cells including HL60 leukemia cells [17], PC-3 human prostate cancer cells [18], HepG2 liver cancer [19], Caco2 human colon cancer [20] and SK-Hep-1 human hepatoma cell [21]. Fucoxanthin was found capable of intervention in signal transduction pathways including *ERK*, *P13 K/AKT* [21], *MAPK* and *p38* inhibition [22] as well as *JAK/STAT* pathway [23]. These cellular signaling pathways ultimately affect gene and protein expression in cancer cell division and apoptosis. More importantly, it was found that fucoxanthin was a better radical scavenger than the ubiquitously sourced beta-carotene; especially in physiological anoxic conditions [24]. Nevertheless, past studies have focused on using purified fucoxanthin compounds which considerably elevates product cost, limits accessibility, and the purification process strips away other functional bioactives present in the microalgal biomass.

Therefore in this study, the crude extract and a fucoxanthin rich fraction derived from it were extracted from the biomass of a tropical marine diatom, *Chaetoceros calcitrans* and compared for their efficacy in inducing anti-proliferation in HepG2 liver cancer cell line. Mixtures of active compounds in the form of rich fractions may have additive or synergistic effects by targeting different cell pathways simultaneously. Moreover, bioactive-rich fractions have been reported to produce better efficacy than their respective single compound [25]. Therefore, this study hypothesized that fucoxanthin-rich fraction (FxRF) would be more effective against HepG2 liver cancer cells than the crude extract.

2. Materials and methods

2.1. Chemicals and reagents

Dichloromethane, methanol and dimethyl sulfoxide (DMSO) were purchased from Merck KGaA (Darmstadt, Germany). Acridine orange (AO) was purchased from Sigma (Sigma-Aldrich, St Louis, MO, USA). RPMI-1640, fetal bovine serum, trypsin, penicillin, propidium iodide (PI), RNase A and 3-(4,5-dimethylthiazol-2-yl)-2,5 diphenyltetrazolium bromide (MTT) were purchased from Nacalai Tesque (Kyoto, Japan). Real Genomics Total RNA extraction kit (RBC Biosciences, Taiwan) and GenomeLab GeXP Start Kit (Beckman Coulter, USA) were procured for this study. Tissue culture flasks and 96-well plates were acquired from TPP (Trasadingan, Switzerland).

2.2. Preparation of crude methanolic extract (CME) and FxRF from Chaetoceros calcitrans *biomass*

Chaetoceros calcitrans culturing conditions and biomass collection followed our previous method [26]. Firstly, the CME was prepared from 10 g of lyophilised biomass mixed with 250 mL methanol. Filtrates from three extractions were pooled and the solvents removed under low pressure (RotaVapor R210, Buchi, Postfach, Flawil, Switzerland). Next, the FxRF was produced via fractionation of the CME to concentrate fucoxanthin and its co-extracts. This was done by dispersing 1.0 g of CME in 25 mL of distilled water followed by the addition of 125 mL of dichloromethane. The mixture was poured into a separating funnel to yield two layers. The organic layer from three extractions was pooled and its solvent was then removed under reduced pressure. All extracts and fractions were stored in a −80 °C freezer prior to analysis. A detailed account for the preparation and characterization of the CME and FxRF can be found from our previous publication [27]

2.3. Cell culture

The human liver cancer cells (HepG2) were purchased from the American Type Culture Collection (ATCC, Manassas, VA, USA) and grown in complete culture medium of Roswell Park Memorial Institute (RPMI) medium (Nacalai Tesque, Kyoto, Japan) supplemented with 10% fetal bovine serum (Sigma-Aldrich, St. Louis, MO, USA) and 1% penicillin (Nacalai Tesque, Kyoto, Japan) and maintained at 37 °C under 5% CO_2 incubator. The stock concentration (100 mg.mL^{-1}) of the extract was prepared in DMSO (Friedemann Schmidt, Francfort, Germany). Also, DMSO concentration was kept under 0.1% for all cell culture assays.

2.4. The cytotoxicity of CME and FxRF

MTT assay (Mosmann 1983) was used to evaluate anti-proliferative properties and efficacies of both CME and FxRF on HepG2 cells. Besides, the effects of the CME and FxRF were tested on 3T3 mouse fibroblast cell line to determine their effects on non-cancerous cells. Doxorubicin (Sigma-Aldrich, St Louis, MO, USA) was used as a positive control in this assay. Each 96-well flat bottom plate was seeded with a concentration of 1×10^4 cells. mL^{-1} and incubated at 37 °C (5% CO_2 and 95% air) for 24 h to allow cell adherence. The cells were treated with the CME (400, 200, 100, 50 μg.mL^{-1}) and FxRF (40, 20, 10, 5 μg.mL^{-1}) for 24 h, 48 h and 72 h. After incubation, each well was added with 20 μL of MTT (5 mg. mL^{-1}) solution and further incubated for 4 h at 37 °C. The supernatant was carefully removed and 100 μL of DMSO was added to dissolve the formazan crystals. Absorbance was measured at 540 nm and a reference wavelength of 630 nm using a microplate reader (Multiskan™ GO UV/Vis microplate spectrophotometer, Thermo Fisher Scientific, USA). Assays were performed in triplicates and in three independent tests. A graph of percentage of cell viability versus concentration of extracts was plotted and the concentration of extracts which inhibited 50% cellular growth compared to control (IC_{50}) was determined.

2.5. Morphological analysis using phase contrast microscopy and acridine orange/propidium iodide staining with fluorescent microscopy

HepG2 cells were seeded at a density of 1×10^4 cells. mL^{-1} in six well culture plates and allowed to attach for 24 h. The next day, cells were treated with respective extracts at selected concentrations (CME: 200, 100, 50 μg.mL^{-1}; FxRF: 40, 20, 10 μg.mL^{-1}) for 72 h. For phase contrast imaging, cells were kept in a stage top-incubator (Tokai-Hit, Japan) and multiple images at the same spot were taken every 24 h for 72 h using an Orca Flash 2.8 monochrome microscope model (Hamamatsu, Japan) at 20× objective using image acquisition software cellSense Dimension v1.12. On the other hand, to observe cell death, cells were prepared the same

way as described in MTT assay. After 24 h treatment incubation, the growth media was discarded and cells were stained with 20 μL dye mixture consisting of 10 μL of 1 mg.mL^{-1} AO (Sigma-Aldrich, St Louis, MO, USA) and 10 μL of 1 mg.mL^{-1} PI (Nacalai Tesque, Kyoto, Japan). Morphological changes and characteristics of apoptosis or necrosis in cells were examined with an inverted fluorescence microscope (Olympus, Tokyo, Japan) where multiple independent images were taken.

2.6. Cell cycle analysis

Cells were seeded in 25 cm^2 T-flasks (1×10^5 cells. mL^{-1}) in 3 mL of complete growth culture media, incubated for 24 h and treated with respective extracts at different time points (24 h, 48 h, and 72 h). Floating cells were collected and adherent cells harvested by trypsinization. All cells were pelleted at 100×g for 5 min. Cells were washed twice in PBS and resuspended in 70% ethanol at −20 °C for 24 h. Prior to data collection with flow cytometry, cells were pelleted, washed once with PBS and resuspended in 425 μL PBS, 25 μL PI (1 mg.mL^{-1}) and 50 μL of RNase A (1 mg.mL^{-1}; Amresco, OH, USA). Cells were left to incubate on ice for 20 min. The distribution of the cell cycle from at least 10,000 cells was measured by a flow cytometer with Summit software (Version 4.3; CyAN ADP, Beckman Coulter: Brea. CA. USA) and data analysis was carried out with ModFit LT software.

2.7. Multiplex gene expression analysis

2.7.1. RNA extraction

Cells were seeded in six well plates (1×10^4 cells. mL^{-1}) in 3 mL of RPMI media. After treatment, floating cells were collected and adherent cells trypsinized to detach cells. Cells were centrifuged at 100×g to obtain pellet and washed twice with PBS. The cell's RNA was isolated using Total RNA Isolation kit (RBC Bioscience Corp., Taiwan) in accordance with manufacturer's protocol. RNA concentration was determined using NanoDrop spectrophotometer (Thermo Scientific Nanodrop, NanoDrop Technologies, Wilmington, DE, USA), and only RNA of good quality based on the A260/280 and A260/A230 ratios (1.8–2.0) was used.

2.7.2. Primer design

Primers were designed on the GenomeLab Xpress Profiler software with *Homo sapiens* sequence from National Centre for Biotechnology Information GenBank Database (http://www.ncbi.nlm.nih.gov/nucleotide/). The genes of interest, housekeeping genes, and internal control are presented in Table 1. The forward and reverse primers had universal tag sequences in addition to nucleotides complementary to target genes. Primers were purchased from First Base Ltd. (Selangor, Malaysia) and diluted in 1 × TE buffer. Primers were stored at −20 °C until use.

2.7.3. Reverse transcription and polymerase chain reaction (PCR)

Reverse transcription (RT) and multiplex PCR of RNA samples (50 ng/μL) were carried out in XP Thermal Cycler (Biometra T personal Thermocycler, Whatman Biometra, Goettingen, Germany) according to GenomeLab™GeXP Start Kit (Beckman Coulter Inc., Miami, FL, USA) with slight modifications. Briefly, RT reaction mixture was prepared using RNA sample (1 μL each), 4 μL of 5 × RT buffer, 2 μL of RT reverse primers, 1 μL of KanR, 1 μL of reverse transcriptase and 11 μL of RNase-free water to make up to 20 μL. cDNA was synthesized according to the reaction protocol: 48 °C/1 min, 42 °C/60 min, 95 °C/5 min, and 4 °C hold using a Thermal cycler machine (Biometra T personal Thermocycler, Whatman Biometra, Goettingen, Germany). Following RT, 9.3 μL of each cDNA was mixed with 10.7 μL of PCR reaction mixture consisting of 4 μL 5 × PCR buffer, 4 μL 25 mM $MgCl_2$, 2 μL PCR forward primer and 0.7 μL of Thermo-Start DNA polymerase. Amplification conditions were 95 °C for 10 min, followed by 35 cycles of 94 °C/30 s, 55 °C/30 s, 70 °C/1 min and 4 °C hold (Biometra T personal Thermocycler, Whatman Biometra, Goettingen, Germany).

2.7.4. GeXP data analysis

PCR products (1 μL each) from the above reactions were mixed with 38.5 μL of sample loading solution and 0.5 μL of DNA size standard 400 (Beckman Coulter Inc, Miami, FL, USA) in a 96 well sample loading plate and analysed on the GeXP machine (Beckman Coulter Inc, Miami, FL, USA). The GeXP system separated PCR product size based on capillary gel electrophoresis. The dye signal strength was measured in arbitrary units (A.U.). The results were analysed using the Fragment Analysis module of the GeXP system software and then imported into the analysis module of eXpress Profiler software. Normalization was performed with β-actin according to the manufacturer's instructions.

3. Statistical analysis

Shapiro-Wilk test was used to check for normality ($p > 0.05$). MTT assay followed a two-way analysis of variance (ANOVA) to compare time and dose-independent variables to cell cytotoxicity using GraphPad Prism 7.0 (GraphPad Prism Software Inc., San Diego, USA). Cell cycle analysis and gene expression followed

Table 1
Gene name, accession number, product size and primer sequences used in the GeXP multiplex analysis of selected genes based on *Homo sapiens* gene sequences adopted from the National Centre for Biotechnology Information. (http://www.ncbi.nlm.nih.gov/nucleotide/).

Gene	Accession number	Forward universal primer sequence	Reverse universal primer sequence
BAX	NM_004324	AGGTGACACTATAGAATAGCAAACTGGTGCTCAA	GTACGACTCACTATAGGGAAACCACCCTGGTCTTG
BCL-2	NM_000633	AGGTGACACTATAGAATACTGTGGATGACTGAGTACCT	GTACGACTCACTATAGGGATCAGAGACAGCCAGGAG
APAF	NM_001160	AGGTGACACTATAGAATACATACTCTTTCACCAGATCA	GTACGACTCACTATAGGGAACAAGTTCTGTTTTTGCTTT
BID	NM_001196	AGGTGACACTATAGAATAGTCTTTCACACAACAGTGA	GTACGACTCACTATAGGGAACACTGGAAGCAGCTATAC
CYCS	NM_018947	AGGTGACACTATAGAATAGAGCGAGTTTGGTTGC	GTACGACTCACTATAGGGAAAATCTTCTTGCCTTTCTC
JNK	NM_139046	AGGTGACACTATAGAATACAGAAGCTCCACCACCAAAGAT	GTACGACTCACTATAGGGAGCCATTGATCACTGCTGCAC
ERK1/2	NM_002745	AGGTGACACTATAGAATAGGAGCAGTATTACGACCCGA	GTACGACTCACTATAGGGAGATGTCTGAGCACGTCCAGT
AKT1	NM_001014431	AGGTGACACTATAGAATAGAGGAGATGGACTTCCGGTC	GTACGACTCACTATAGGGAAGGATCTTCATGGCGTAGTAGC
ACTIN B[a]	NM_001101	AGGTGACACTATAGAATAGATCATTGCTCCTCCTGAGC	GTACGACTCACTATAGGGAAAAGCCATGCCAATCTCATC
GAPDH[a]	NM_002046	AGGTGACACTATAGAATAAAGGTGAAGGTCGGAGTCAA	GTACGACTCACTATAGGGAGATCTCGCTCCTGGAAGATG
KAN[b]	KANr	AGGTGACACTATAGAATAATCATCAGCATTGCATTCGATTCCTGTTTG	GTACGACTCACTATAGGGAATTCCGACTCGTCCAACATC
SOD1	NM_000454	AGGTGACACTATAGAATATCATCAATTTCGAGCAGAAGG	GTACGACTCACTATAGGGATGCTTTTTCATGGACCACC
SOD2	NM_000636	AGGTGACACTATAGAATACATCAAACGTGACTTTGGTTC	GTACGACTCACTATAGGGACTCAGCATAACGATCGTGGTT
CAT	NM_001752	AGGTGACACTATAGAATAGAAGTGCGGAGATTCAACACT	GTACGACTCACTATAGGGAACACGGATGAACGCTAAGCT

[a] House keeping genes.
[b] Internal control, * Gene used for normalization. Underlined sequences are universal tags.

oneway ANOVA in which Tukey HSD post hoc test was selected to analyze the difference between treatment means (SPSS 21.0, SPSS Inc., Chicago, USA). Values were expressed as the mean ± SD from three independent experiments (n = 3).

4. Results and discussion

4.1. FxRF and CME is cytotoxic to human liver HepG2 cancer cells but not to 3T3 non-cancerous cells

Fig. 1 shows both extracts demonstrating cytotoxicity by inhibiting proliferation of HepG2 cancer cells; measured using MTT assay. A significant interaction effect ($p < 0.05$) between time and dose was observed in both treatments as validated by the two way ANOVA analysis. In particular, treatment dosage with only $18.89 \pm 0.06\ \mu g.mL^{-1}$ of FxRF yielded the same inhibitory activity (IC_{50}) than treatment dosage of $87.5 \pm 0.01\ \mu g.mL^{-1}$ of CME; after 72 h. The 4.6 times increase in IC_{50} may be contributed by FxRF having 4.2 fold more fucoxanthin i.e. 84.62 ± 0.28 mg $FX.g^{-1}$ extract compared to CME that only contained 20.12 ± 0.12 mg $FX.g^{-1}$ extract (Table 3). A similar pattern was previously accounted where in vitro antioxidant capacities too were elevated [27]. The significantly higher anti proliferative potency in FxRF compared to CME could have been contributed by the difference in fucoxanthin concentration upon a fractionation procedure.

Table 2 shows the cytotoxic effects of an anti-cancer drug, doxorubicin on HepG2 cells where IC_{50} for doxorubicin at 72 h was $0.85 \pm 0.04\ \mu g.mL^{-1}$. Although doxorubicin was more potent, it is important to note that the doxorubicin used was in its pure form. Additionally, past report found fucoxanthin to exhibit additive or synergistic effects when used in combination with drug compounds like cisplatin [21]. From here, fucoxanthin can be used to complement existing drug compounds for enhanced efficacy. In this case, the potency of FxRF may be a product of additive or synergistic effect between fucoxanthin and gallic acid in the rich fraction. We previously proved that rich fractions have better efficacies in antioxidant properties [25,27].

The selection of the 3T3 cell line was based on testing recommendations (NIH Pub no. 01-4499) (National Institute of Environmental Health Sciences 2001) for the effect of drugs and extracts on non-cancerous cells. It was found that treatment with CME and FxRF did not show cytotoxic effects on 3T3 non-cancerous cells at concentrations below $200\ \mu g.mL^{-1}$ and $100\ \mu g.mL^{-1}$ respectively. As a matter of fact, only a small dose of *C. calcitrans* extracts was enough to inhibit the proliferation of HepG2 cancer cells compared to 3T3 non-cancerous cells. For example, CME at a concentration of $87.50 \pm 0.01\ \mu g.mL^{-1}$ was needed to inhibit the growth of 50% of HepG2 cancer cells as opposed to $350.00 \pm 0.26\ \mu g.mL^{-1}$ needed to kill 50% non-cancerous 3T3 fibroblast cells. Similarly, FxRF ($18.89 \pm 0.06\ \mu g.mL^{-1}$) inhibited proliferation of HepG2 cells whereas 3T3 cells grew normally despite treatment at a concentration as high as $100\ \mu g.mL^{-1}$. Besides, it is recommended in subsequent studies to test the produced extracts on other cancer cells to compare if similar effects on HepG2 cells are observed.

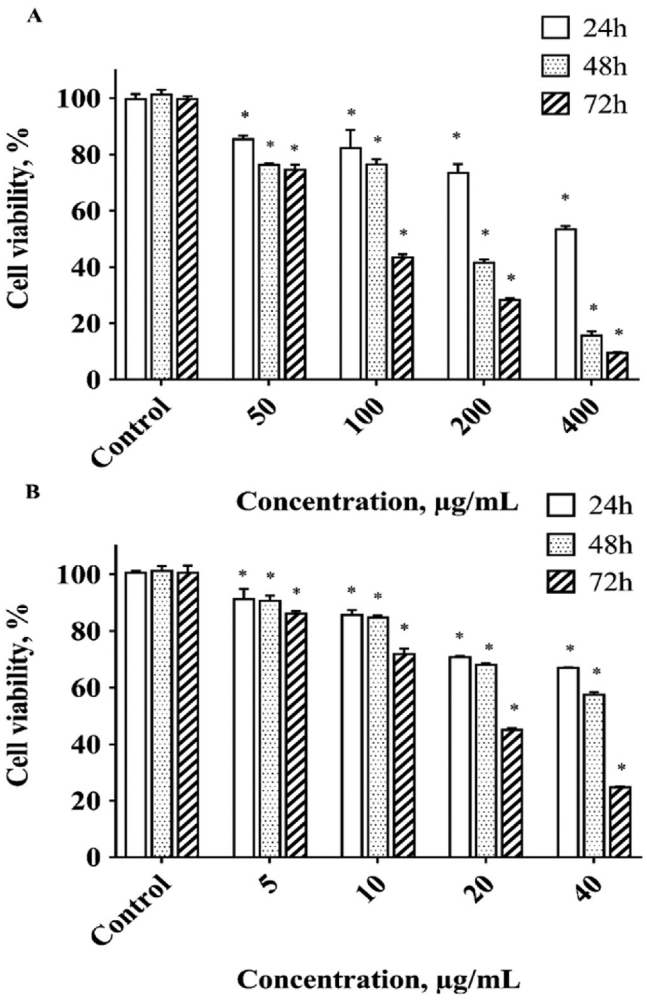

Fig. 1. Increasing cytotoxic effects of *Chaetoceros calcitrans* extract on HepG2 cell line after 24, 48 and 72 h treated by (a) CME at 50, 100, 200, 400 $\mu g.mL^{-1}$; (b) FxRF at 5, 10, 20, 40 $\mu g.mL^{-1}$. Data are presented as mean ± SD (n = 3). * significantly different from the control ($p < 0.05$).

FxRF exacerbate apoptosis vs. CME: Morphological analysis with phase contrast microscopy and AO/PI staining with fluorescent microscopy

In this qualitative visualization section, phase contrast images of treated and untreated HepG2 cells were captured using a live cell imaging system on a time-dependent manner using IC_{50} values of both CME and FxRF extracts for a 72 h duration. Whereas, fluorescence microscopy using AO/PI double staining dyes on HepG2 cells followed a dose-dependent manner in which cells were treated at a series of concentrations for 24 h.

From the phase contrast microscopy images, the morphological changes were evident in extract treated cells as compared to untreated cells. It was determined that the growth inhibition of HepG2 cells by CME treatment (Fig. 2a) and FxRF treatment

Table 2
Mean IC_{50} values of CME, FxRF, and doxorubicin in HepG2 and 3T3 cell lines (n = 3).

	Half-maximal inhibitory concentration, IC_{50} ($\mu g.mL^{-1}$)		
	24 h	48h	72h
CME treated HepG2	400	200	87.5
FxRF treated HepG2	80	40	18.9
Doxorubicin treated HepG2	1.25	1.0	0.8
CME treated 3T3 cells	>500	>400	350
FxRF treated 3T3 cells	>100	>100	>100

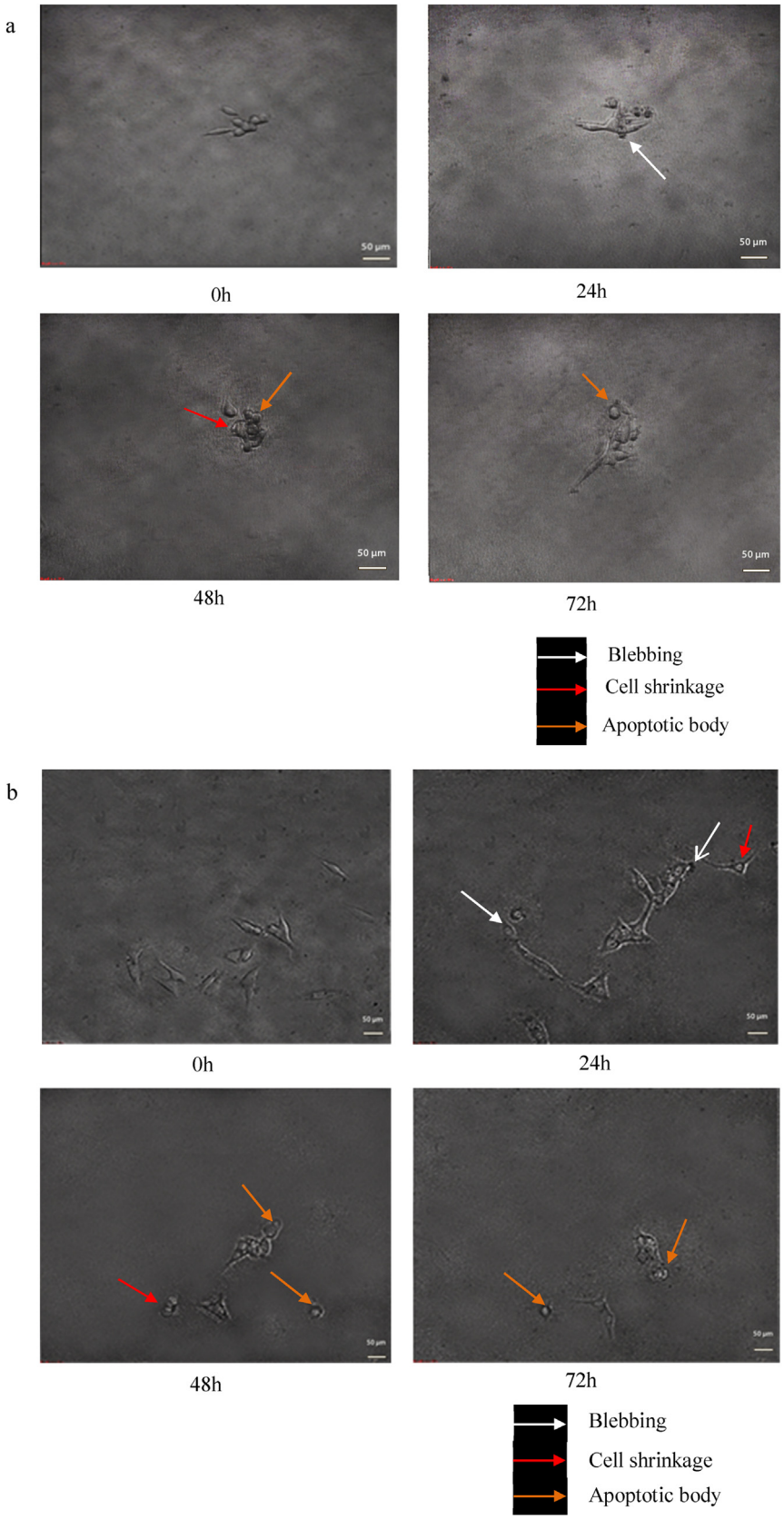

Fig. 2. a Representative phase contrast micrographs of HepG2 cells treated with *Chaetoceros calcitrans* crude methanolic extracts (CME) at 100 μg.mL^{-1} at 24 h intervals. Cells showed increasingly distinctive hallmarks of apoptosis (cell shrinkage, membrane blebbing and formation of pro-apoptotic bodies) with time. Fig. 2b Representative phase contrast micrographs of HepG2 cells treated with FxRF at 20 μg.mL^{-1} at 24 h intervals. FxRF treated cells showed more apoptotic occurrences as compared to CME treated cells.

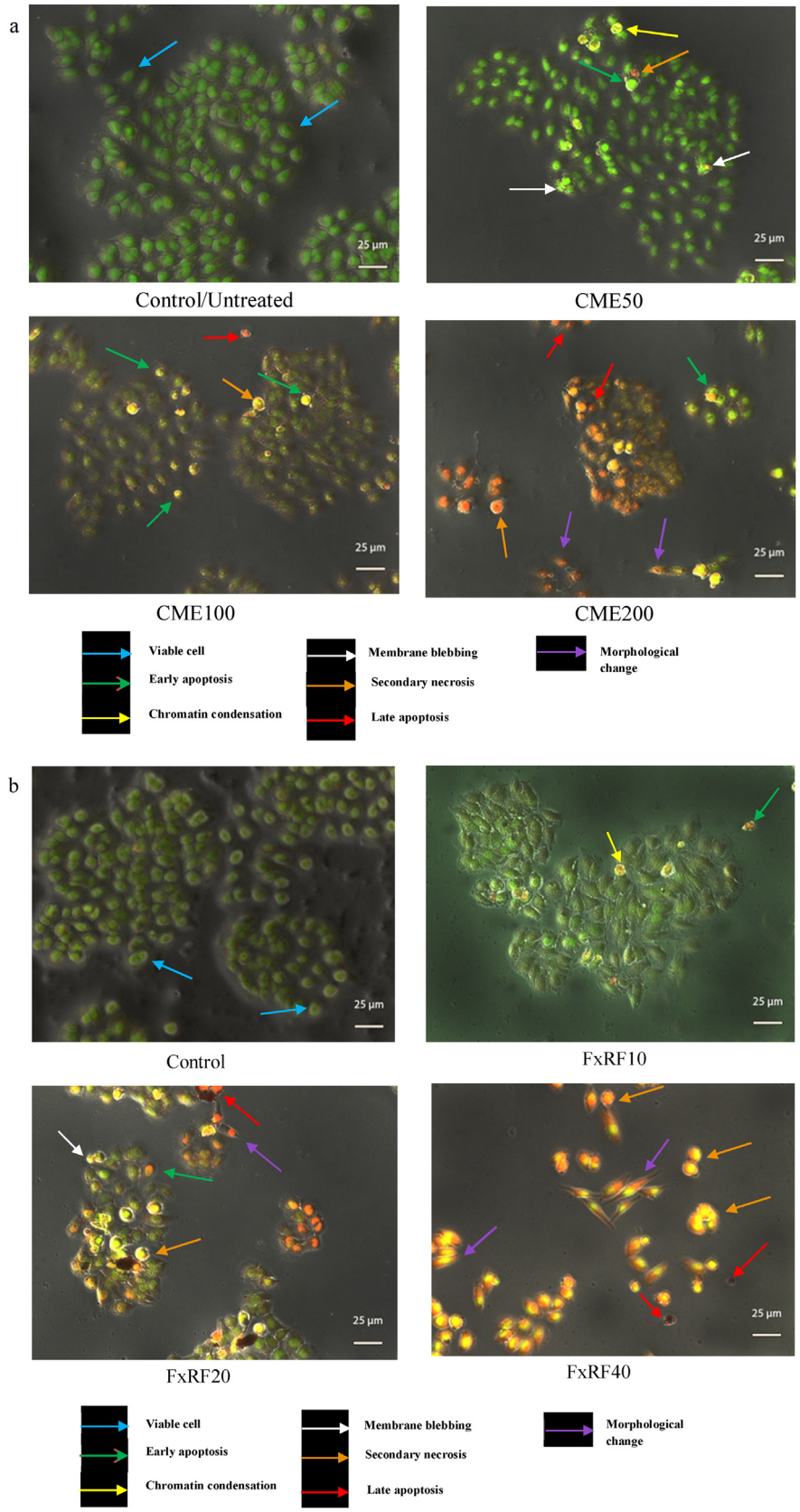

Fig. 3. a Representative fluorescent micrographs of HepG2 cells double-stained with acridine orange and propidium iodide after treatment for 24 h with crude methanolic extracts (CME: 200, 100, 50 µg.mL^{-1}). Control cells showed viable cells with no prominent apoptosis; CME50 showed early apoptosis represented by membrane blebbing and bright yellow chromatin condensation; CME100 displayed frequent signs of early apoptosis and proceeding to secondary necrosis; CME200 showed more signs of late apoptosis, secondary necrosis and morphological changes from round to spindle-shaped cells. Fig. 3b Representative fluorescent micrographs of HepG2 cells double-stained with acridine orange and propidium iodide after treatment for 24 h with fucoxanthin rich fraction (FxRF: 40, 20, 10 µg.mL^{-1}). Control cells showed intact

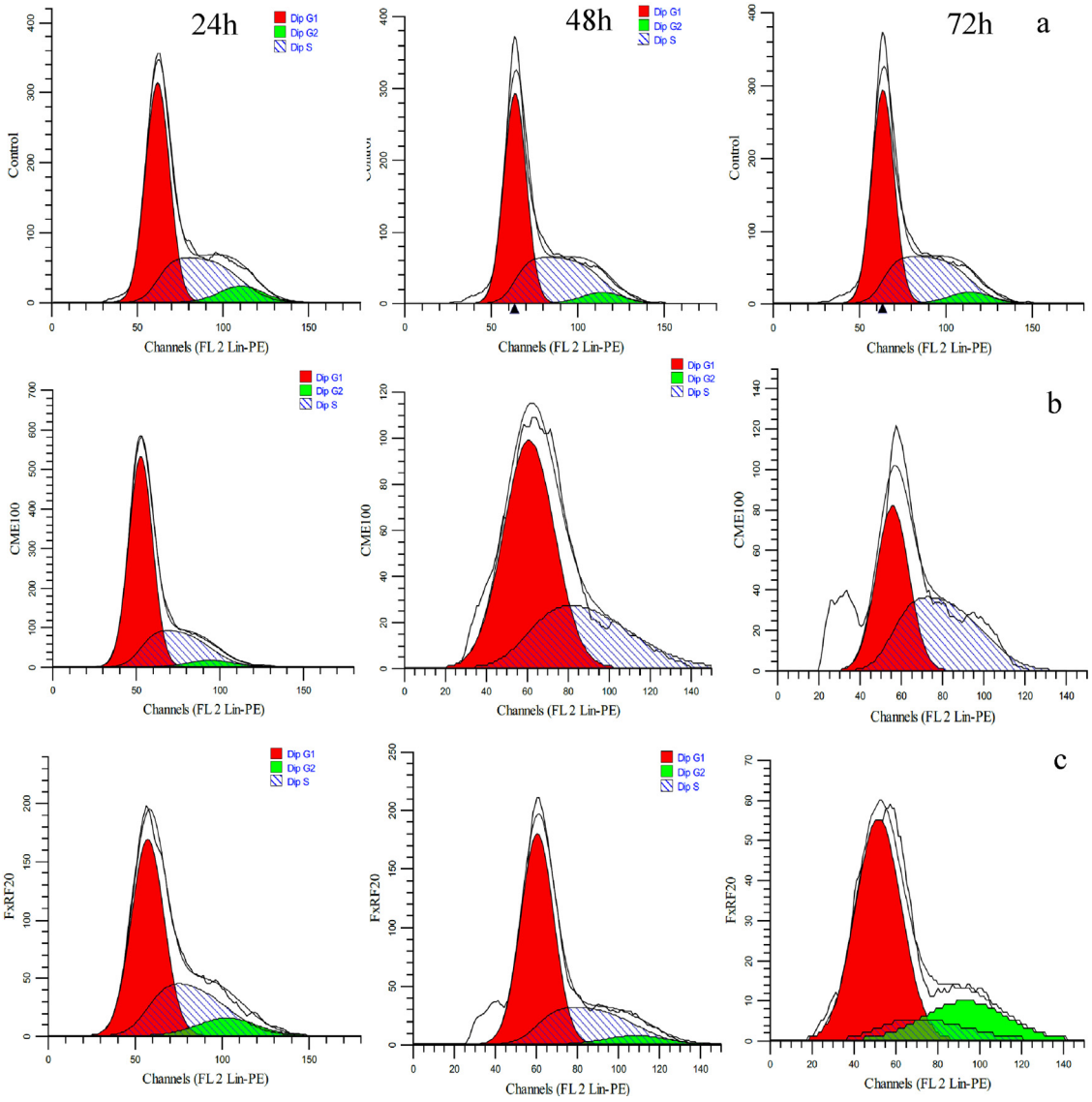

Fig. 4. Representative cell cycle histograms of (a) control; (b) CME treated cells and; (c) FxRF treated cells after 24, 48 and 72 h.

(Fig. 2b) followed an apoptotic mechanism. This was based on observations of apoptotic hallmarks i.e. cell shrinkage and fragmentation to smaller compartments like membrane-bound apoptotic bodies. For example, untreated cells remained confluent throughout incubation period, whilst treated cells shrunk in sizes with cell membrane detachment from the monolayer surface. Chromatin condensation, cell blebbing and apoptotic body formation were also observed to occur frequently in the treated cells as compared to untreated cells.

AO/PI stains were intercalating nucleic acid-specific fluorochromes which emitted green and orange fluorescence respectively. PI was only able to cross compromised cell membranes which enabled discrimination between viable and dead cells. The hallmarks of apoptosis included chromatin condensation, cell shrinkage, multi-nucleation, abnormalities of mitochondrial cristae, membrane blebbing, holes, cytoplasm extrusions and formation of apoptotic bodies; collectively confirmed by AO/PI double staining [28]. Cells with green nuclei with intact structure were identified as viable whereas, early apoptotic cells exhibited bright and dense green chromatin; late apoptotic cells showed dense orange areas of chromatin condensation and secondary necrotic cells had orange nuclei with intact structure [29]. Untreated and treated cells stained with AO/PI are shown in Fig. 3a and b. It was found that treated-cells exhibited apoptotic hallmarks whereas the untreated cells remained confluent with intact nuclei throughout the incubation period.

Overall, it was observed that FxRF-treated cells showed a higher apoptotic effect compared to CME. This was supported by higher chromatin aggregation at the nuclear membrane, distinct cell membrane detachment from monolayer surface and onset of chromatin condensation. This was in agreement with previous findings on the appearance of membrane blebs, DNA condensation, and fragmentation as significant signs of apoptosis [30]. For future studies, it is recommended that the apoptosis induction property of FxRF be validated using Annexin-V assay to further support the result obtained in AO/PI assay.

cytoplasm and round viable nuclei with some late apoptosis; FxRF10 showed chromatin condensation, early apoptosis with initial morphological changes; FxRF20 exhibited higher numbers of early apoptotic cells as well as late apoptosis; FxRF40 showed the most occurrence of late apoptosis, secondary necrosis, and distinctive cell morphological changes.

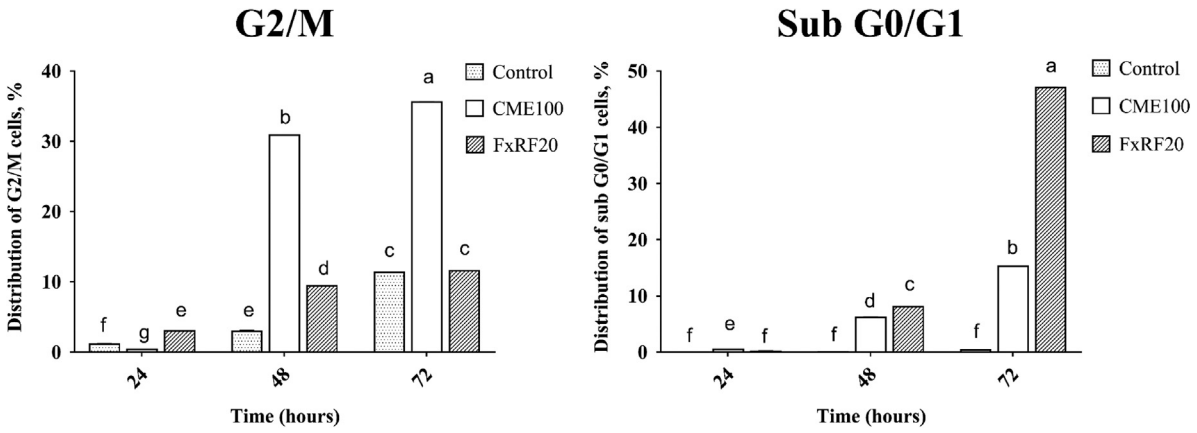

Fig. 5. The inhibition of HepG2 cell growth via cell cycle arrest at G2/M phase and apoptosis at sub G0/G1. Data are presented as mean ± SD (n = 3). Different letters on bars indicate significant difference ($p < 0.05$) between treatments and treatment time. FxRF treated cells significantly induced apoptosis as shown in DNA accumulation at sub G0/G1 phase as compared to CME treated cells.

4.2. FxRF induces sub G0/G1 DNA accumulation while CME arrest cells at G2/M phase

Fig. 4 shows a representative histogram of DNA accumulation in different cell cycle phases. CME treatment caused a significantly higher cell accumulation at G2/M phase (0.39%→30.87%→35.57%) with time as compared to control cells and FxRF treated cells. FxRF treated cells induced cell arrest at G2/M phase 3.01% (24 h) →9.39% (48 h) →11.57% (72 h). This observation agreed with previous studies reporting fucoxanthin treated cells to undergo G2/M cell cycle arrest [12,23].

Furthermore, the sub G0/G1 phase accumulation is an index for apoptotic DNA and nuclei fragmentation [31]. Results showed that treated cells significantly accumulated at the sub G0/G1 phase compared to untreated cells in a time-dependent manner. From 24 h to 72 h, CME treated cells gathered at the sub G0/G1 phase (0.48%→6.17%→15.25%) whilst FxRF treated cells (0.16%→8.04%→47.04%) were at a higher extent than CME. These findings corroborated with a previous study where cells accumulated at sub G1 (72.75 ± 1.23%) at 72 h in MCF7 breast cancer cells when treated with *C. calcitrans* ethanolic extracts [32].

By the 72nd hour, a large proportion of CME treated cells arrested at the G2/M checkpoint but did not proceed to mitosis stage where cells divided into two (Fig. 5). Whereas FxRF treated cells accumulated at sub G0/G1 resting stage; preventing cells from entering S phase. A quick comparison between FxRF and CME showed FxRF treatment (47.04%) resulted in approximately 3.08 times higher cell accumulation at sub-G0/G1 as compared to CME treatment (15.25%). This can be accounted for by the higher amount of fucoxanthin in FxRF than CME (Table 3).

4.3. CME and FxRF treatment alters the mRNA levels of cell signaling, apoptotic and antioxidant genes

Gene expression of CME and FxRF treated HepG2 cells were observed in a time-dependent manner in an effort to elucidate mRNA regulations in anti-proliferative activity (Fig. 6). Firstly, the signaling genes (*AKT1, ERK1/2,* and *JNK*) gene expression level in the CME-treated and FxRF-treated HepG2 cells were downregulated in a time-dependent manner. For example, CME treatment suppressed *AKT1* expression by 1.66 folds i.e. from 1.08 ± 0.01 (24 h) to 0.65 ± 0.05 (72 h). More than CME, FxRF treatment inhibited *AKT1* expression by 2.58 folds i.e. from 1.16 ± 0.03 (24 h) to 0.45 ± 0.00 (72 h). Previous studies have demonstrated that apoptosis was closely linked with the inhibition of the *AKT* signaling pathway [33,34] and it has been one of the targeted pathways in cancer treatment [35]. Besides, *ERK1* and *ERK2* were the central components of the MAPK (mitogen-activated protein kinase) cascade, involved in growth and differentiation. By down-regulation of the expression of *ERK1/2* genes, DNA replication was inhibited therefore leading to cancer cell death [36]. In this regard, findings were in agreement with previous studies [37,38]. Also, *JNK* functions to directly phosphorylate *Bcl-2* (B-cell CLL/Lymphoma-2) to enable co-localizing and collaborating with *Bcl-2* to mediate prolonged cell survival [39]. Increased expressions of *JNK* and *Bcl-2* in cancer cells were not desirable, and as such cancer cell proliferation could be inhibited if this pathway was modulated [40,41]. Accordingly, both extracts significantly downregulated *JNK* expression with FxRF exhibiting a significantly higher down-regulating effect than CME treatment ($p < 0.05$).

Secondly, the expression data from the apoptotic study were different between CME and FxRF extracts. CME treated cells suggested favourable apoptotic promoter effects based on the upregulation of *BAX* and *BID* gene and inhibition of expression of the anti-apoptotic *Bcl-2* gene; by the 48th hour. Meanwhile, FxRF treated cells did not significantly change the regulation of pro-apoptotic and anti-apoptotic levels but affected the cells through elevation of *APAF* and *CYCS* expression as shown in more than 1 fold increase compared to CME at the 72nd hour. Upregulation in *CYCS* gene expression resulted in the activation of caspase-9 and caspase-3 cascade in turn leading to apoptosis [42].

Table 3
Fucoxanthin concentration in extracts. Highest peak appearance observed at the same elution time as standard confirming fucoxanthin as a lead compound. At the same concentration, FxRF had a higher fucoxanthin content (mg FX. g^{-1} extract) compared to CME.

Details/Extract	Fucoxanthin standard	Crude methanolic extract (CME)	Fucoxanthin-rich fraction (FxRF)
Concentration (μg. ml^{-1})	625	1000	1000
HPLC elution time (minute)	7.030	7.032	7.017
Fucoxanthin concentration in extract (mg FX. g^{-1} extract)	n/a	20.12 ± 0.12	84.62 ± 0.28

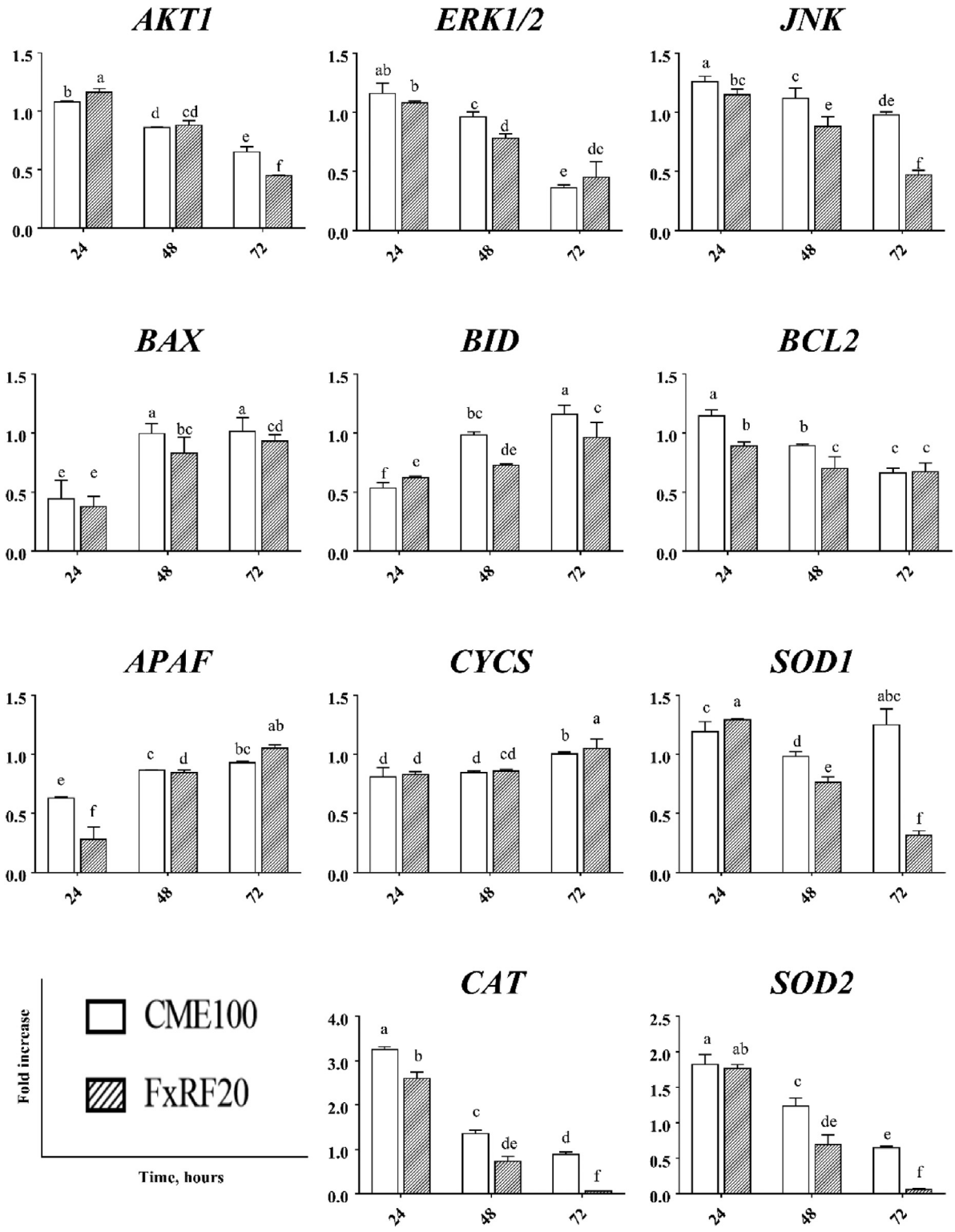

Fig. 6. mRNA expression levels post-treatment with CME at 100 μg.mL^{-1} and FxRF at 20 μg.mL^{-1}. The analysis was focused on the expression of upstream signaling genes (*AKT*1; *ERK*1/2; *JNK*); apoptosis-related genes (*BAX*; *Bcl2*; *BID*; *APAF*, *CYCS*); and antioxidant genes (*SOD1*, *SOD2*, *CAT*). Fold changes was normalized against beta-actin where >1 indicate upregulation and <1 indicate downregulation. Data are presented as mean ± SD of three independent tests. Different letters on bars indicate a significant difference between treatments and treatment time ($p < 0.05$).

Downregulation of antioxidant genes in cancer cells indicates a failure to protect itself *i.e*. a favourable treatment effect. *SOD* and *CAT* are enzymes that neutralize free radical species and are involved in oxidative stress regulation [43]. The initial high levels of the antioxidant gene expression in the HepG2 cells were likely an indication of the cell's survival mechanism against oxidative stress-induced apoptotic death. In the third set of genes investigated, it was found that treatment with both types of microalgae extracts significantly downregulated the expression of antioxidant genes (SOD2 and CAT) in a time-dependent manner.

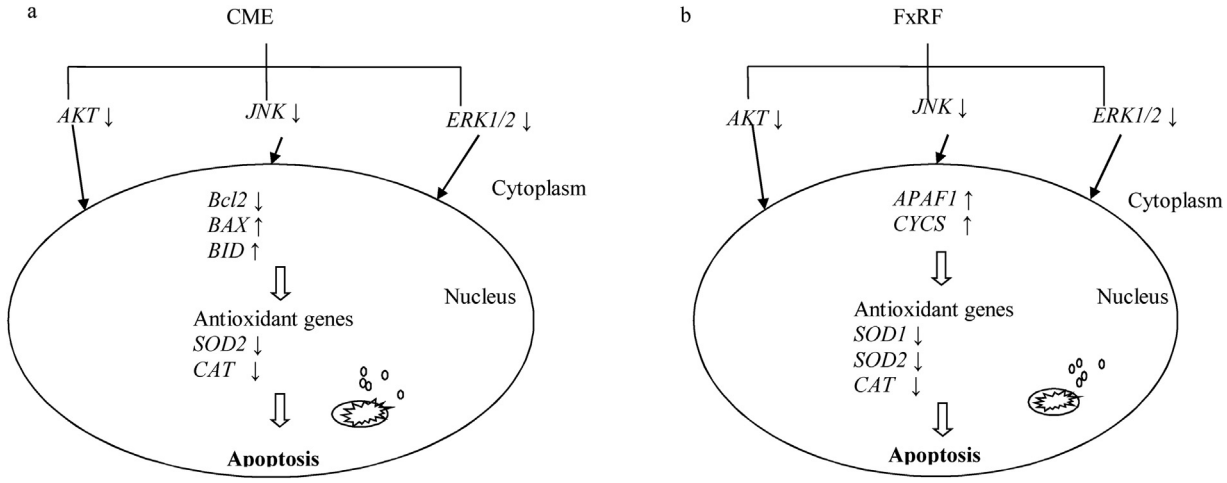

Fig. 7. Proposed schematic diagram of the pro-apoptotic mechanism of (a) CME and (b) FxRF extracts from *C. calcitrans* in HepG2 cancer cells.

For example, *CAT* expression was significantly reduced 3.65 folds i.e. 3.25 ± 0.07 (24 h) to 0.89 ± 0.05 (72 h) when treated with CME. More so, FxRF treatment significantly decreased ($p < 0.05$) *CAT* expression by 18.6 folds i.e. from 2.60 ± 0.14 (24 h) to 0.06 ± 0.00 (72 h). In other words, the cellular antioxidative capacity in the cancer cells was reduced post-treatment. As a result, reduced antioxidant status coupled with an inability to scavenge radicals increased oxidative stress leading to cancer cell death through apoptosis [44,45]. Our finding supported an earlier report demonstrating the role of fucoxanthin in oxidative stress [46].

Regulation of gene expression by redox state has been one of the promising therapeutic approaches involved in cancer therapy [47,48]. It is worthy to highlight FxRF demonstrated a significantly higher ($p < 0.05$) efficacy compared to CME on the 3rd day. Indeed, the act of fractionation may have concentrated other bioactive compounds besides fucoxanthin which accounted for the higher efficacy. Further compound elucidation in our study [26] identified gallic acid as the major phenolic acid present in *C. calcitrans*.

Overall, the gene expression data showed that treatment with extract stimulated changes in the signaling, apoptotic and oxidative stress genes thereby altering signaling patterns in the cell resulting in cell death. Cellular oxidative stress could result in the death of cells through induction of apoptosis, a process important in the removal of cancerous cells. In the event that endogenous control cannot induce oxidative stress to remove cells, exogenous agents are often used to induce enough oxidative stress that will lead to apoptotic cell removal. In fact, this has been the focus of many potential anti-cancer agents [49,50]. For example, the red algae, *Acanthophora spicifera* exhibiting a similar effect on cancer cells through the down-regulation of *Bcl-2* expression [9]. The multiple target pathway of action for *C. calcitrans* is illustrated in Fig. 7.

5. Conclusion

Treatment using *Chaetoceros calcitrans* extracts successfully resulted in HepG2 cancer cell death via apoptotic pathway; the desirable means of cancer cell cytotoxicity. Notably, the anti-proliferative activity was found to be enhanced significantly in FxRF compared to CME. This implied that an increase in fucoxanthin concentration accounted for the enhanced apoptotic activity in cancer cells. G2/M cell cycle arrest was observed after treatment with FxRF inducing higher sub G0/G1 cell accumulation; a proxy of apoptosis. Finally, gene expression analysis revealed that extract cytotoxicity towards HepG2 cell line was mediated through multiple signaling pathways which transcriptionally regulated apoptotic cell death. Overall, *C. calcitrans* can be a sustainable source of natural compounds with potentially good anti-cancer effects.

Author contributions

SCF performed experiments, interpreted the data and prepared the manuscript under the supervision of FMY and MI. FMY, NKMH, and JBF critically revised the manuscript. MUI, NHA, NI, and YST contributed to GeXP analysis and data interpretation. All authors take responsibility for the integrity of the work as a whole, from inception to finished article.

Conflict of interest

The authors declare no conflicts and informed consent.

Acknowledgements

The authors acknowledge the financial support of the Malaysia Ministry of Higher Education for Fundamental Research Grant Scheme (FRGS: 02-01-13-1224FR), SATREP−COSMOS matching fund and Higher Institutions Centre of Excellence (HiCOE: 6369100) Research Fund. More than that, the authors would like to dedicate this research article to the memory of the late Prof Dr. Mahiran Basri who is greatly missed.

References

[1] M.C.S. Wong, J.Y. Jiang, W.B. Goggins, M. Liang, Y. Fang, F.D.H. Fung, C. Leung, H. H.X. Wang, G.L.H. Wong, V.W.S. Wong, International incidence and mortality trends of liver cancer: a global profile, Sci. Rep. 7 (2017) 45846 %@ 42045-42322.
[2] P.C. Valery, M. Laversanne, P.J. Clark, J.L. Petrick, K.A. McGlynn, F. Bray, Projections of primary liver cancer to 2030 in 30 countries worldwide, Hepatology 67 (2018) 600-611 %@ 1527-3350.
[3] R. Verpoorte, Good practices: the basis for evidence-based medicines, J. Ethnopharmacol. 140 (2012) 455–457.
[4] K. Shinkai, H. Akedo, M. Mukai, F. Imamura, A. Isoai, M. Kobayashi, I. Kitagawa, Inhibition of in vitro tumor cell invasion by ginsenoside Rg3, Jpn. J. Cancer Res. 87 (1996) 357–362.
[5] A.P. Sutter, K. Maaser, P. Grabowski, G. Bradacs, K. Vormbrock, M. Höpfner, A. Krahn, B. Heine, H. Stein, R. Somasundaram, Peripheral benzodiazepine receptor ligands induce apoptosis and cell cycle arrest in human hepatocellular carcinoma cells and enhance chemosensitivity to paclitaxel, docetaxel, doxorubicin and the Bcl-2 inhibitor HA14-1, J. Hepatol. 41 (2004) 799–807.
[6] S. Ibsen, E. Zahavy, W. Wrasdilo, M. Berns, M. Chan, S. Esener, A novel doxorubicin prodrug with controllable photolysis activation for cancer chemotherapy, Pharm. Res. 27 (2010) 1848–1860.

[7] N.R. Farnsworth, The role of ethnopharmacology in drug development. Bioactive compounds from plants, Ciba Found. Symp. (1990) pp. 2–11 discussion 11.

[8] T.F. Molinski, D.S. Dalisay, S.L. Lievens, J.P. Saludes, Drug development from marine natural products, Nat. Rev. Drug Discov. 8 (2009) 69–85.

[9] V.K. Sali, R. Malarvizhi, V.M. Manikandamathavan, H.R. Vasanthi, Isolation and evaluation of phytoconstituents from red alga Acanthophora spicifera as potential apoptotic agents towards A549 and HeLa cancer cells lines, Algal Res. 32 (2018) 172-181 %@ 2211-9264.

[10] A.M.S. Mayer, K.B. Glaser, C. Cuevas, R.S. Jacobs, W. Kem, R.D. Little, J.M. McIntosh, D.J. Newman, B.C. Potts, D.E. Shuster, The odyssey of marine pharmaceuticals: a current pipeline perspective, Trends Pharmacol. Sci. 31 (2010) 255–265.

[11] N. Sithranga Boopathy, K. Kathiresan, Anticancer drugs from marine flora: an overview, J. Oncol. (2010).

[12] S.R. Kumar, M. Hosokawa, K. Miyashita, Fucoxanthin: a marine carotenoid exerting anti-cancer effects by affecting multiple mechanisms, Mar. Drugs 11 (2013) 5130–5147.

[13] K. Yamamoto, C. Ishikawa, H. Katano, T. Yasumoto, N. Mori, Fucoxanthin and its deacetylated product, fucoxanthinol, induce apoptosis of primary effusion lymphomas, Cancer Lett. 300 (2011) 225–234.

[14] S.C. Foo, F.M. Yusoff, M. Ismail, M. Basri, S.K. Yau, N.M.H. Khong, K.W. Chan, M. Ebrahimi, Antioxidant capacities of fucoxanthin-producing algae as influenced by their carotenoid and phenolic contents, J. Biotechnol. 241 (2017) 175-183 %@ 0168-1656.

[15] D. Pádua, E. Rocha, D. Gargiulo, A.A. Ramos, Bioactive compounds from brown seaweeds: phloroglucinol, fucoxanthin and fucoidan as promising therapeutic agents against breast cancer, Phytochem. Lett. 14 (2015) 91-98 %@ 1874-3900.

[16] P. Rajendran, N. Nandakumar, T. Rengarajan, R. Palaniswami, E.N. Gnanadhas, U. Lakshminarasaiah, J. Gopas, I. Nishigaki, Antioxidants and human diseases, Clin. Chim. Acta 436 (2014) 332–347.

[17] K.N. Kim, S.J. Heo, S.M. Kang, G. Ahn, Y.J. Jeon, Fucoxanthin induces apoptosis in human leukemia HL-60 cells through a ROS-mediated Bcl-xL pathway, Toxicol. Vitr. 24 (2010) 1648–1654.

[18] E. Kotake-Nara, A. Asai, A. Nagao, Neoxanthin and fucoxanthin induce apoptosis in PC-3 human prostate cancer cells, Cancer Lett. 220 (2005) 75–84.

[19] S.K. Das, T. Hashimoto, K. Kanazawa, Growth inhibition of human hepatic carcinoma HepG2 cells by fucoxanthin is associated with down-regulation of cyclin D, Biochim. Biophys. Acta (BBA) – Gen. Subj. 1780 (2008) 743–749.

[20] M. Hosokawa, M. Kudo, H. Maeda, H. Kohno, T. Tanaka, K. Miyashita, Fucoxanthin induces apoptosis and enhances the antiproliferative effect of the PPARγ ligand, troglitazone, on colon cancer cells, Biochim. Biophys. Acta (BBA) – Gen. Subj. 1675 (2004) 113–119.

[21] C.L. Liu, Y.P. Lim, M.L. Hu, Fucoxanthin enhances cisplatin-induced cytotoxicity via NFκB-mediated pathway and downregulates DNA repair gene expression in human hepatoma HepG2 cells, Mar. Drugs 11 (2013) 50–66.

[22] Y. Satomi, H. Nishino, Implication of mitogen-activated protein kinase in the induction of G1 cell cycle arrest and GADD45 expression by the carotenoid fucoxanthin in human cancer cells, Biochim. Biophys. Acta (BBA) – Gen. Subj. 1790 (2009) 260–266.

[23] R.X. Yu, X.M. Hu, S.Q. Xu, Z.J. Jiang, W. Yang, Effects of fucoxanthin on proliferation and apoptosis in human gastric adenocarcinoma MGC803 cells via JAK/STAT signal pathway, Eur. J. Pharmacol. 657 (2011) 10–19.

[24] T. Nomura, M. Kikuchi, A. Kubodera, Y. Kawakami, Proton-donative antioxidant activity of fucoxanthin with 1,1-diphenyl-2-picrylhydrazyl (DPPH), Biochem. Mol. Biol. Int. 42 (1997) 361–370.

[25] M.U. Imam, M. Ismail, D.J. Ooi, N.H. Azmi, N. Sarega, K.W. Chan, M.I. Bhanger, Are bioactive-rich fractions functionally richer? Crit. Rev. Biotechnol. (2015) 1–9.

[26] S.C. Foo, F.M. Yusoff, M. Ismail, M. Basri, N.M.H. Khong, K.W. Chan, S.K. Yau, Efficient solvent extraction of antioxidant-rich extract from a tropical diatom, Chaetoceros calcitrans (Paulsen) Takano 1968, Asian Pac. J. Trop. Biomed. 5 (2015) 834–840.

[27] S.C. Foo, F.M. Yusoff, M. Ismail, M. Basri, S.K. Yau, N.M.H. Khong, K.W. Chan, Production of fucoxanthin-rich fraction (FxRF) from a diatom, Chaetoceros calcitrans (Paulsen) Takano 1968, Algal Res. 12 (2015) 26–32.

[28] S.I. Abdel Wahab, A.B. Abdul, A.S. Alzubairi, M. Mohamed Elhassan, S. Mohan, In vitro ultramorphological assessment of apoptosis induced by zerumbone on (HeLa), J. Biomed. Biotechnol. (2009) article ID: 769568.

[29] G. Ciapetti, D. Granchi, L. Savarino, E. Cenni, E. Magrini, N. Baldini, A. Giunti, In vitro testing of the potential for orthopedic bone cements to cause apoptosis of osteoblast-like cells, Biomaterials 23 (2002) 617–627.

[30] N.H. Azmi, N. Ismail, M.U. Imam, M. Ismail, Ethyl acetate extract of germinated brown rice attenuates hydrogen peroxide-induced oxidative stress in human SH-SY5Y neuroblastoma cells: role of anti-apoptotic, pro-survival and antioxidant genes, BMC Complement. Altern. Med. (2013) 13.

[31] Y. Chen, E. McMillan-Ward, J. Kong, S.J. Israels, S.B. Gibson, Oxidative stress induces autophagic cell death independent of apoptosis in transformed and cancer cells, Cell Death Differ. 15 (2008) 171–182.

[32] S. Ebrahimi Nigjeh, F.M. Yusoff, N.B. Mohamed Alitheen, M. Rasoli, Y.S. Keong, A.R.B. Omar, Cytotoxic effect of ethanol extract of microalga, Chaetoceros calcitrans, and its mechanisms in inducing apoptosis in human breast cancer cell line, Biomed. Res. Int. 2013 (2013).

[33] G. Ye, Q. Lu, W. Zhao, D. Du, L. Jin, Y. Liu, Fucoxanthin induces apoptosis in human cervical cancer cell line HeLa via PI3K/Akt pathway, Tumor Biol. 35 (2014) 11261–11267.

[34] J.S. Yoon, E.S. Kim, B.B. Park, J.H. Choi, Y.W. Won, S. Kim, Y.Y. Lee, Anti-leukemic effect of sodium metaarsenite (KML001) in acute myeloid leukemia with breaking-down the resistance of cytosine arabinoside, Int. J. Oncol. 46 (2015) 1953–1962.

[35] Y. Yu, F. Bai, Y. Liu, Y. Yang, Q. Yuan, D. Zou, S. Qu, G. Tian, L. Song, T. Zhang, Fibroblast growth factor (FGF21) protects mouse liver against d-galactose-induced oxidative stress and apoptosis via activating Nrf2 and PI3K/Akt pathways, Mol. Cell. Biochem. (2015) 1–13.

[36] F. Gan, Z. Zhang, Z. Hu, J. Hesketh, H. Xue, X. Chen, S. Hao, Y. Huang, P.C. Ezea, F. Parveen, Ochratoxin A promotes porcine circovirus type 2 replication in vitro and in vivo, Free Radic. Biol. Med. 80 (2015) 33–47.

[37] A. Cumaoglu, S. Dayan, A.O. Agkaya, Z. Ozkul, N.K. Ozpozan, Synthesis and pro-apoptotic effects of new sulfonamide derivatives via activating p38/ERK phosphorylation in cancer cells, J. Enzyme Inhib. Med. Chem. (2014) 1–7.

[38] Y. Wang, Q. Tu, W. Yan, D. Xiao, Z. Zeng, Y. Ouyang, L. Huang, J. Cai, X. Zeng, Y.-J. Chen, CXC195 suppresses proliferation and inflammatory response in LPS-induced human hepatocellular carcinoma cells via regulating TLR4-MyD88-TAK1-mediated NF-κB and MAPK pathway, Biochem. Biophys. Res. Commun. 456 (2015) 373–379.

[39] Q.H. Wu, Z.H. Yuan, X.J. Zhang, The cell survival function of JNK, Mil. Med. Sci. Lett. 83 (2014) 28–33.

[40] A. Malki, R.Y. Elbayaa, H.M.A. Ashour, C.A. Loffredo, A.M. Youssef, Novel thiosemicarbazides induced apoptosis in human MCF-7 breast cancer cells via JNK signaling, J. Enzyme Inhib. Med. Chem. (2014) 1–10.

[41] X. Yang, X. Xiang, M. Xia, J. Su, Y. Wu, L. Shen, Y. Xu, L. Sun, Inhibition of JNK3 promotes apoptosis induced by BH3 mimetic S1 in chemoresistant human ovarian Cancer cells, Anat. Rec. 298 (2015) 386–395.

[42] P. Li, D. Nijhawan, I. Budihardjo, S.M. Srinivasula, M. Ahmad, E.S. Alnemri, X. Wang, Cytochrome c and dATP-dependent formation of Apaf-1/caspase-9 complex initiates an apoptotic protease cascade, Cell 91 (1997) 479–489.

[43] I. Fridovich, Superoxide radical and superoxide dismutases, Annu. Rev. Biochem. 64 (1995) 97–112.

[44] P. Collins, C. Jones, S. Choudhury, L. Damelin, H. Hodgson, Increased expression of uncoupling protein 2 in HepG2 cells attenuates oxidative damage and apoptosis, Liver Int. 25 (2005) 880–887.

[45] S.P. Hussain, P. Amstad, P. He, A. Robles, S. Lupold, I. Kaneko, M. Ichimiya, S. Sengupta, L. Mechanic, S. Okamura, L.J. Hofseth, M. Moake, M. Nagashima, K.S. Forrester, C.C. Harris, p53-induced up-regulation of MnSOD and GPx but not catalase increases oxidative stress and apoptosis, Cancer Res. 64 (2004) 2350–2356.

[46] C.L. Liu, Y.T. Chiu, M.L. Hu, Fucoxanthin enhances HO-1 and NQO1 expression in murine hepatic BNL CL. 2 cells through activation of the Nrf2/ARE system partially by its pro-oxidant activity, J. Agric. Food Chem. 59 (2011) 11344–11351.

[47] J. Chandra, A. Samali, S. Orrenius, Triggering and modulation of apoptosis by oxidative stress, Free Radic. Biol. Med. 29 (2000) 323–333.

[48] J.M. Matés, J.A. Segura, F.J. Alonso, J. Márquez, Oxidative stress in apoptosis and cancer: an update, Arch. Toxicol. 86 (2012) 1649–1665.

[49] S. Azam, N. Hadi, N.U. Khan, S.M. Hadi, Prooxidant property of green tea polyphenols epicatechin and epigallocatechin-3-gallate: implications for anticancer properties, Toxicol. Vitro 18 (2004) 555–561.

[50] C.A. de la Lastra, I. Villegas, Resveratrol as an antioxidant and pro-oxidant agent: mechanisms and clinical implications, Biochem. Soc. Trans. 35 (2007) 1156–1160.